HHS Public Access

Author manuscript

ACS Chem Biol. Author manuscript; available in PMC 2019 January 03.

Published in final edited form as:

ACS Chem Biol. 2018 September 21; 13(9): 2808–2818. doi:10.1021/acschembio.8b00759.

Reprogramming a Deubiquitinase into a Transamidase

Lin Hui Chang[†] and **Eric R. Strieter**[*,†,‡]

[†]Department of Chemistry, University of Massachusetts-Amherst, Amherst, Massachusetts 01003, United States

[‡]Department of Biochemistry and Molecular Biology, University of Massachusetts-Amherst, Amherst, Massachusetts 01003, United States

Abstract

Access to well-defined ubiquitin conjugates has been key to elucidating the biochemical functions of proteins in the ubiquitin signaling network. Yet, we have a poor understanding of how deubiquitinases and ubiquitin-binding proteins respond to ubiquitin modifications when anchored to a protein other than ubiquitin or a ubiquitin-like protein. This is due to the difficulty of synthesizing ubiquitinated proteins comprised of native isopeptide bonds. Here we report on the evolution of a deubiquitinase capable of site-specifically modifying itself with defined ubiquitin chains. Following mutagenesis and yeast display screening, we identify a variant of the yeast ubiquitin C-terminal hydrolase Yuh1 that has a 28-fold improvement in the transamidation to hydrolysis ratio relative to the wild type enzyme. The switch in activity enables robust autoubiquitination of a lysine in the crossover loop to form an isopeptide bond. We demonstrate the utility of autoubiquitinating the evolved Yuh1 variant by investigating the consequences of ubiquitin chain anchoring on the activities of other deubiquitinases. Much to our surprise, we find that certain deubiquitinases are exquisitely sensitive to chain anchoring. These results highlight the importance of investigating the biochemical activities of deubiquitinases with both substrate-anchored and unanchored ubiquitin chains.

Graphical Abstarct

[*]**Corresponding Author:** estrieter@chem.umass.edu.

Supporting Information

The Supporting Information is available free of charge on the ACS Publications website at DOI: 10.1021/acschembio.8b00759. Supporting methods; *Yuh*1cDNA sequence (Table S1); primers used in this study (Table S2); MALDI-TOF calibration curve for Ub WT and Ub allylamine (Figure S1); Western blot analysis of the autoubiquitination of Yuh1 variants (Figure S2); gel replicates for autoubiquiti-nation of Yuh1qm variants (Figure S3); gel replicates of the cleavage of Yuh1qm5.6-anchored and unanchored chains by USP11 (Figure S4); gel replicates of the cleavage of Yuh1qm5.6-anchored and unanchored chains by USP15 (Figure S5); gel replicates of the cleavage of Yuh1qm5.6-anchored and unanchored chains by USP21 (Figure S6); cleavage of non-NEM treated Yuh1qm5.6-anchored K48 Ub dimers by USP15 (Figure S7); cleavage of Yuh1qm5.6-anchored K48 Ub dimers by OTUB1-UBE2D2 (Figure S8); LC-MS/MS data for autoubiquiti-nation on K66 (Table S3 and S6), K163 (Table S4 and S7) and K164 (Table S5 and S8); sequencing data for yeast display-based directed evolution for the initial library (Table S9), after three rounds of selection (Table S10), and after five rounds of selection (Table S11) (PDF)

Table S3: Yuh1qm Mono-ubiquitination site identified through in gel digestion by trypsin and GluC (XLSX)

Table S4: Yuh1qm ubiquitination site identified through in solution digestion by trypsin and GluC (XLSX)

Table S5: Yuh1qm5.6 ubiquitination site identified through in solution digestion by trypsin and GluC (XLSX)

Table S6: MS/MS peak list for peptide with K66 ubiquitination (XLSX)

Table S7: MS/MS peak list for peptide with T163K ubiquitination (XLSX)

Table S8: MS/MS peak list for peptide with N163K ubiquitination (XLSX)

The authors declare no competing financial interest.

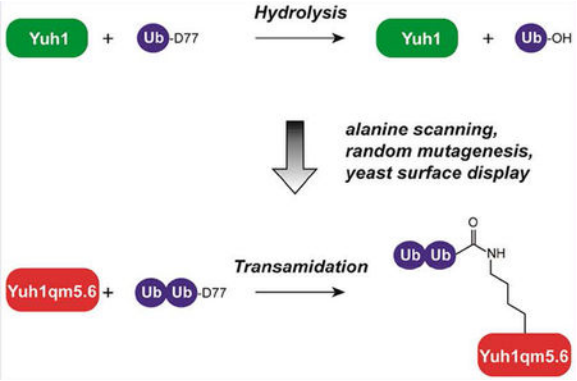

Nearly every biochemical pathway in eukaryotes is regulated by covalent attachment of ubiquitin to other proteins including itself.[1,2] As a result, aberrancies in ubiquitination or deubiquitination are often associated with human disease.[2] The biological impact of ubiquitin has therefore led to a great deal of interest in dissecting the biochemical functions of proteins involved in the ubiquitin network.[3] To facilitate these efforts, chemical and enzymatic methods have been developed to generate ubiquitin activity-based probes, ubiquitin-peptide and ubiquitin-protein conjugates, including a variety of ubiquitin chains with defined linkages and lengths.[4–7] These tools have been instrumental in defining the biochemical functions of E3 ubiquitin ligases,[8] deubiquitinases/DUBs,[9] and proteins with ubiquitin binding domains (UBDs).[10]

Despite advances made with designer ubiquitin conjugates, pressing questions remain regarding the influence of ubiquitinated proteins on the specificities of DUBs and UBDs. To what extent do different substrate proteins contribute to the specificities of DUBs and UBDs? Does anchoring a ubiquitin chain to a substrate alter the reactivity or binding properties of DUBs and UBDs? Addressing these issues is challenging using chemical and enzymatic approaches to synthesize substrate-anchored ubiquitin conjugates.[11–13] The ligation chemistry required for the generation of an isopeptide bond involves incorporating a 1,2-aminothiol into a substrate protein;[14–20] however, the thiol must be removed to unveil a native linkage.[21,22] Moreover, denaturing conditions necessary for optimal ligation and subsequent desulfurization often preclude the formation of functional ubiquitin-protein conjugates. With existing enzymatic methods, it is difficult to control the type of ubiquitin modification and the extent to which a substrate is modified.[23–25]

We envisioned building ubiquitin-protein conjugates using a DUB to install defined ubiquitin modifications on itself. Although this approach is restricted to generating ubiquitinated DUB conjugates, proteomic studies have shown that most DUBs (there are ~100 in humans) are extensively ubiquitinated in cells,[26] and the functional consequences are often poorly understood.[27] Moreover, reprogramming a DUB to generate defined ubiquitin-protein conjugates is conceptually new. Instead of using ATP, E1, and an E2 to activate ubiquitin as an acyl adenylate and subsequently generate a high energy thioester intermediate that is then used to build ubiquitin-protein conjugates, predefined ubiquitin variants carrying a genetically encoded C-terminal extension are reacted with a DUB and

transferred to a lysine residue. A native isopeptide bond can therefore be forged between defined ubiquitin chains and a DUB without the need for chemical synthesis.

As the model system for exploring whether a DUB can ubiquitinate itself, we chose the yeast ubiquitin C-terminal hydrolase Yuh1. We have previously shown that at alkaline pH Yuh1 reacts with ubiquitin conjugates containing a single C-terminal amino acid extension (typically D77) to generate an acyl-enzyme intermediate that can be intercepted by amine nucleophiles.[28–30] With wild type Yuh1 the problem is that hydrolysis is still an order of magnitude faster than aminolysis.[30] To transform Yuh1 into an enzyme capable of modifying itself with ubiquitin and ubiquitin chains, it is necessary to improve its transamidase activity.

Here, using an integrated approach of alanine scanning, random mutagenesis, and yeast surface display screening we demonstrate that Yuh1 can be engineered into a transamidase capable of installing a variety of ubiquitin chains on a single lysine residue. By interrogating different DUBs with autoubiquitinated Yuh1 variants we observe cases in which cleavage of an anchored chain occurs with markedly different efficiency than the unanchored version. These results not only demonstrate that DUBs are sensitive to the type of substrate attached to the chain, but also underscore the importance of investigating the biochemical activities of DUBs with both substrate-anchored and unanchored ubiquitin chains.

RESULTS AND DISCUSSION

Targeted Mutagenesis.

In earlier studies, we found that Yuh1 could be used to append amines to the C-terminus of mono-Ub and Ub chains through a transamidation reaction at pH 10.4.[30] Thus, we needed to improve the transamidation to hydrolysis ratio in order to transform Yuh1 into an enzyme capable of ubiquitinating itself.

We decided to pursue a targeted mutagenesis approach centered on residues near the active site. As a guide we turned to the extant structure of monoUb-bound Yuh1.[31] The structure shows a flexible crossover loop that occludes the catalytic residues C90, H166, and D181. This loop undergoes dramatic conformational changes to accommodate the ubiquitin C-terminus in the active site. Key to stabilizing the loop in a more open conformation is N88 (Figure 1A). The invariant N88 is also positioned to provide transition state stabilization by forming an oxyanion hole. The β4-β5 loop of Yuh1 houses the catalytic D181 involved in proton transfer steps. We replaced residues in each of these regions with alanine to measure their impact on both hydrolysis and transamidation.

To monitor reactions with each Yuh1 variant, we availed a MALDI-TOF mass spectrometric-based assay originally developed for deubiquitinases.[32] The amounts of hydrolysis and transamidation products were quantitated using ^{15}N-labeled Ub as an internal standard (Figures 1B and S1). With allylamine as the nucleophile and Ub-D77 as the substrate, we found that Yuh1 N88A and the N88A/D162A/L165A (NDL) triple mutant display significantly higher transamidase activity at pH 8 compared to the wild type enzyme. The Yuh1 NDL variant (herein referred to as Yuh1m) affords Ub-allylamine in an ~30%

yield after an hour (Figure 1C), whereas the transamidation product can barely be detected using the wild type enzyme. A more comprehensive examination of Ala mutants shows the triple mutants N88A/S154A/L165A (NSL) and Yuh1m furnish an ~30% yield of Ub-allylamine, and a transamidation to hydrolysis ratio of 1 and 3, respectively (Figure 1C,D). Substitutions within the $\beta4-\beta5$ loop also transform Yuh1 into a transamidase, though they are not as effective as the other Ala variants. Together, these results indicate that Ala substitutions at Asn88 and within the crossover loop significantly improve the transamidation activity of Yuh1.

To provide more insight into the improved activity, we performed initial rate measurements. As anticipated due to its proposed role in Michaelis complex formation and transition state stabilization,[33] the replacement of N88 with Ala significantly impairs the hydrolase activity of Yuh1 (Figure 2; Table 1). Compared to wild type Yuh1, the k_{cat} drops by 50-fold to 0.06 s^{-1} and the K_m increases by 7-fold to 27 μM, resulting in a 300-fold decrease in catalytic efficiency. The transamidase activity is also adversely affected by the N88A substitution; the k_{cat} decreases by 10-fold and the K_m increases by 4-fold relative to the wild type enzyme. The net result is that hydrolysis and transamidation now have the same catalytic efficiencies. These data also reveal that the hydrolysis reaction is markedly more sensitive to the N88A substitution than transamidation, particularly in the rate of catalytic turnover. A similar trend is observed with Yuh1m; again, the overall activity is compromised relative to wild type, but transamidation is still capable of effectively competing with hydrolysis (Figure 2B; Table 1). In fact, moving from N88A to Yuh1m affords the same turnover rate (0.3 s^{-1}) but the K_m is lowered by 2.5-fold, resulting in a slightly higher efficiency for transamidation relative to hydrolysis (~1.2-fold) (Figure 2C; Table 1). Together, these results demonstrate that just a few mutations near the active site of Yuh1 can compromise the rate of hydrolysis to the extent that transamidation begins to prevail.

Autoubiquitination.

Having found a variant of Yuh1 capable of catalyzing transamidation with a higher efficiency than hydrolysis, we wanted to investigate whether it could undergo autoubiquitination. Yuh1 is a member of the ubiquitin C-terminal hydrolase (UCH) family of DUBs and proteomic studies have shown that all of the human UCHs are ubiquitinated within the flexible crossover loop.[26] We sought to mimic this type of ubiquitination by introducing a Lys in the crossover loop of Yuh1m. Hence, we decided to replace T163 with Lys, as the crystal structure shows the side chain of the former points toward the catalytic Cys (Figure 1A).[31] The resulting quadruple mutant N88A/D162A/T163K/L165A (termed Yuh1qm) was mixed with ubiquitin D77. Within 5 min, free Yuh1qm decreases in abundance, which coincides with the generation of three higher molecular weight species (Figure 3A). The most intense band (band 1) migrates at an apparent molecular weight consistent with the addition of a single Ub to Yuh1qm. Band 2 appears at a slightly higher molecular weight than band 1; however, it is not a molecular weight consistent with two Ub units on Yuh1qm. Band 3 matches a Yuh1qm variant modified with two Ub molecules (see below). These same species were not detected with wild type Yuh1, the T163K single mutant, or Yuh1m. Western blot analysis confirmed the presence of Ub in each of the higher molecular weight species (Figure S2).

To identify the conjugation sites by mass spectrometry, we performed an in-gel digest with a combination of trypsin and GluC. We detected two peptides bearing a diGly-modified Lys, one containing the expected Lys, K163, and another with K66 (Figure 3B; Tables S3 and S6), in each of the bands. K66 is located in a region of Yuh1 that is poorly resolved by crystallography and on the opposite side of the primary Ub binding pocket. Because autoubiquitination of K66 is observed with Yuh1qm and to a lesser extent with the parent Yuh1m variant, its abundance must be affected by the T163K substitution. Regardless of whether K66 or K163 is modified, these results demonstrate autoubiquitination will occur when hydrolysis is impaired and there is a Lys side chain in the vicinity of the active site.

Next, we wanted to test whether preassembled Ub chains could be used. Combining Yuh1qm with K48- and K63-linked Ub dimers results in rapid autoubiquitination (Figure 3C). MS analysis of the purified conjugates shows that, unlike reactions with mono-Ub, K163 is the only Lys residue ubiquitinated (Figure 3D; Tables S4 and S7). While these results indicate that Yuh1qm can be site-specifically modified with defined ubiquitin chains, extended reaction times with lower concentrations of ubiquitin reveal that hydrolysis eventually takes over (Figure 3E). In fact, the measured half-life for Ub-Yuh1qm is only 160 ± 60 s when the ubiquitin concentration is 2 μM (Figures 3E and S3) instead of 50 μM (Figure 3D).

Directed Evolution of Yuh1qm.

Because the poor stability precluded us from obtaining sufficient quantities of autoubiquitinated Yuh1qm, we turned our attention to evolving an enzyme less prone to removing ubiquitin modifications from itself. Through random mutagenesis we created a library of variants based on the Yuh1qm scaffold. We then selected for improved autoubiquitination capabilities using a yeast cell surface display platform.[34,35] Briefly, yeast cells expressing an HA-tagged Yuh1qm library as fusions to the cell surface protein Aga2p are treated with biotin-labeled ubiquitin D77. The logic is that if a cell expresses a Yuh1 variant capable of undergoing autoubiquitination via a transamidation reaction with ubiquitin D77, it will become labeled with biotin (Figure 4A). Cells that are both biotinylated and displaying a Yuh1qm variant are enriched by a stepwise process of binding streptavidin- and antibody-fluorophore conjugates and sorting using fluorescence-activated cell sorting (FACS). As validation of this protocol, we displayed both wild type Yuh1 and Yuh1qm on the yeast cell surface, demonstrating that only cells expressing Yuh1qm are capable of efficiently labeling themselves with biotinylated ubiquitin (Figure 4B).

For the library of Yuh1qm variants we used a broad, unbiased approach to generate diversity. We randomized the Yuh1qm gene using an error-prone polymerase to obtain ~10^7 variants with 1−3 mutations per gene (Table S9). After transformation of this library, five rounds of selection were performed with each successive round containing a lower concentration of biotin-labeled ubiquitin D77. We also used either wild type Yuh1 or the Yuh1qm variant-expressing cells from the preceding round to define the FACS gate for isolating improved variants.

After three rounds, we observed a marked increase in the Alexa Fluor 488 signal, indicating higher levels of autoubiquiti-nation (Figure 4C). Sequencing of several clones revealed a

conserved mutation of N164K, which is part of the crossover loop and adjacent to T163K (Figure 5A; Table S10). Consistent with the surface display results, monoubiquitinated Yuh1qm N164K (referred to as Yuh1qm3.1) is significantly more robust than the modified form of Yuh1qm (Figures 5B and S3). Indeed, hydrolysis of autoubiquitinated Yuh1qm3.1 could barely be detected after an hour. Although the carboxamide side chain of N164 points away from the active site,[31] we surmised that perhaps Yuh1qm3.1 is ubiquitinated on N164K instead of T163K (Figure 5A), which might explain the improved stability, as the C-terminus of ubiquitin would no longer be in proximity to the catalytic Cys, thereby reducing the potential for hydrolysis. Mass spectrometric analysis supports this supposition; N164K is the only site of ubiquitination that could be detected (Figure 5C; Tables S5 and S8).

Additional mutations (V86F/L, L139M, V52L, and I202F) were found along with N164K after two more rounds of selection. These substitutions form pairwise interactions in two distinct regions: one near the catalytic Cys residue (residues 86 and 139) and one distant from the active site (residues 52 and 202) (Figure 5A; Table S11). We selected one substitution from each pair to test in autoubiquitination reactions. The resulting variants, Yuh1qm5.1 (Yuh1qm V86F/N164K) and Yuh1qm5.3 (Yuh1qm V52L/N164K), undergo ubiquitination to a slightly greater extent than Yuh1qm3.1 (Figures 5B and S3). Combining V52L and V86F results in the most active autoubiquitinating enzyme (a variant referred to as Yuh1qm5.6) of all the variants tested. Within seconds of mixing with ubiquitin D77, close to 90% of Yuh1qm5.6 is converted into the ubiquitinated form, whereas with Yuh1qm3.1 only a 40% yield is obtained (Figures 5B and S3). On the basis of initial rate measurements, V52L/V86F also improves transamidation reactions with small amine nucleophiles by 28-fold relative to wild type Yuh1 (Figure 2D; Table 1).

Despite dramatic improvements in the initial autoubiquitination yield, autohydrolysis still occurs. As evidenced by gel-based assays, the abundance of the autoubiquitinated products of all round five variants decreases over time (Figures 5B and S3). While quantification of the decay reveals half-lives of 1400 ± 100, 500 ± 100, and 800 ± 100 s, for Ub-Yuh1qm5.1, Ub-Yuh1qm5.3, and Ub-Yuh1qm5.6, respectively, the amounts of Ub-Yuh1qm5.1 and Ub-Yuh1qm5.6 present after an hour are approximately the same as Ub-Yuh1qm3.1 (~40%). Ub-Yuh1qm5.3 has a much faster decay rate, resulting in a 10% yield after an hour, similar to Ub-Yuh1qm. These results demonstrate that the evolved Yuh1 variants have 3- to 9-fold greater stability in their autoubiquitinated form relative to the parent Yuh1qm.

Because the stabilities of autoubiquitinated Yuh1qm3.1, Yuh1qm5.1, and Yuh1qm5.6 are sufficient for biochemical studies with DUBs, in principle each of these variants could be used. However, we found that Yuh1qm5.6 routinely affords higher autoubiquitination yields than the other variants when N-ethylmaleimide (NEM) is added to prevent hydrolysis. On the basis of these results we decided to move forward with Yuh1qm5.6 as a substrate scaffold for ubiquitination.

Chain Anchoring Affects DUB Activity.

To understand how the activities of DUBs are affected by anchoring ubiquitin chains to a protein, we modified Yuh1qm5.6 with K48 and K63 ubiquitin dimers. Both NEM-treated and untreated conjugates were analyzed. We followed the extent of chain cleavage by the

disappearance of diUb-Yuh1qm5.6 and the concomitant appearance of monoUb-Yuh1qm5.6 in gel-based assays. Gels were stained with SYPRO Ruby, but Western blotting with the α-His antibody proved more reliable for quantitative purposes, as it provided an accurate assessment of all 6xHis-tagged Yuh1qm5.6 species. Cleavage efficiencies were directly compared to unanchored dimers using similar concentrations of substrates in each assay.

We profiled DUBs in both the ubiquitin specific protease (USP) and ovarian tumor (OTU) families.[9] All of the USPs tested, USP11, USP15, and USP21, cleave dimers anchored to Yuh1qm5.6 with similar efficiencies as the unanchored forms (Figures 6A,B and S4–S6). USP11 and USP15 appear to hydrolyze unanchored K48 dimers faster than anchored chains. Yet, when K48 chains are not treated with NEM, the rates of hydrolysis are approximately the same (Figure S7). Interestingly, none of the USPs remove monoubiquitin from Yuh1qm5.6, suggesting there is specificity toward the modified substrate. These results are inconsistent with a previous study showing that mono- and di-Ub is readily removed from heterogeneous mixtures of ubiquitinated proteins[13] and imply that if a USP cannot cleave ubiquitin from a substrate protein, it can process the anchored chain from the distal end.

OTUB1 and OTUB2 are highly selective DUBs. OTUB1 exclusively cleaves K48-linked ubiquitin chains and OTUB2 exhibits selectivity toward both K48 and K63 chains.[32,36] Thus, as expected, unanchored dimers are readily processed by both enzymes (Figure 6C). Surprisingly, however, anchoring K48 dimers to Yuh1qm5.6 completely abrogates cleavage by OTUB1 and OTUB2. K63 dimers are cleaved to some extent by OTUB2 when attached to Yuh1qm5.6, but not as efficiently as the unanchored dimers. The lack of activity is not due to inhibition by Yuh1qm5.6 (Figure S8), as unanchored chains are still cleaved by OTUB1 in the presence of diubiquitinated Yuh1qm5.6, nor is it due to NEM treatment. Because E2 conjugating enzymes enhance the activity of OTUB1, we also tested the fusion protein OTUB1-UBE2D2 with anchored and unanchored chains.[37] Like OTUB1 alone, however, OTUB1-UBE2D2 is unable to cleave chains attached to Yuh1qm5.6.

We then thought that perhaps OTUB1 is unable to access both ubiquitin subunits in the dimer, thus we extended the chain attached to Yuh1qm5.6 to a K48 trimer and K6/K48 branched trimer. Once again, we detected little activity. These data therefore suggest that OTUB1, and to a lesser extent OTUB2, has difficulty cleaving a preferred chain type when anchored to certain substrates. Examining the extant structures of OTUB1 bound to ubiquitin aldehyde and a chemical UBE2D2 ~ ubiquitin conjugate reveals that a substrate attached to the proximal subunit of a K48 chain could sterically block the chain from interacting with OTUB1.[37]

In this study, we used a DUB, specifically, a variant of the yeast ubiquitin C-terminal hydrolase Yuh1, to modify itself with defined ubiquitin chains and investigate how other DUBs respond to chain anchoring. Previous efforts to install defined ubiquitin modifications on a protein of interest have focused on chemical and enzymatic approaches using the ubiquitin conjugation machinery. Reprogramming Yuh1 into an enzyme capable of transferring ubiquitin and ubiquitin chains onto a Lys of itself therefore represents a conceptually new approach. To transform Yuh1 into a ligase, we used both targeted and random mutagenesis along with a yeast surface display selection strategy to select for

variants with improved ratios of transamdiation to hydrolysis. This led to the identification of a Yuh1 variant exhibiting a ratio of catalytic efficiencies for transamidation and hydrolysis that is 28-fold higher than the wild type enzyme. Through this approach, we were also able to identify a Lys residue (N164K) that when ubiquitinated is less prone to autohydrolysis. Autoubiquitination of Yuh1 variants provided us with a means to probe the activities of other DUBs with anchored ubiquitin chains. We discovered that DUBs in the OTU family (e.g., OTUB1 and OTUB2) are unable to cleave chains when anchored to the Yuh1 variant. This result is surprising, as the prevailing view is that OTU enzymes such as OTUB1 and OTUB2 largely operate on ubiquitin chains while ignoring the substrate to which they are attached.[38] Our results therefore suggest that the nature of ubiquitinated substrate could play a more important role in regulating the activities of DUBs than currently appreciated.

METHODS

Transamidation Activity Assay.

Transamidation reactions were carried out in a buffered solution containing 50 mM HEPES pH 8.0, 1 mM EDTA, 100 mM allylamine (Sigma-Aldrich), 750 μM Ub D77, and 1 μM enzyme. The reactions were quenched with a solution containing 25 mM iodoacetamide (IAA) and 10% (v/v) acetic acid. Reactions were monitored by MALDI-TOF MS as described below.

MALDI-TOF MS Sample Preparation and Analysis.

To 1 μL of quenched sample was added 1 μL of uniformly ^{15}N-labeled Ub D77 (5 μM). The resulting mixture was then added to 2 μL saturated sinapic acid in 40% acetonitrile, 0.1% TFA. Two microliters of this mixture was then spotted on a 96-ground steel MALDI target plate. MS spectra were acquired on a Bruker MALDI-TOF microflex. For each spectrum, we collected a total of 1000 shots at 45% laser power. Data processing was performed using FlexAnalysis software (Bruker). Calibration curves were obtained for wild type Ub and Ub allylamine to quantify the amount of hydrolysis and transamidation products.

Measuring Kinetics of Yuh1 Mutants Using HPLC.

Kinetic assays were carried out at RT in buffered solution containing 50 mM HEPES pH 8.0, 1 mM EDTA, 100 mM allylamine, and either 7.5 nM wild type Yuh1, or 500 nM of the Yuh1 N88A and Yuh1m variants. Initial rates were measured by varying the concentration of fluorescein-labeled Ub D77. Reactions were quenched at three different time points (0, 1, and 2 min). The fluorescein-labeled components (Ub D77, wild type Ub, and Ub allylamine) were then resolved by HPLC using a cationic exchange column (TOSOH Bioscience) and a buffer containing 25 mM NH_4OAc pH 4.4. A linear gradient of 0.15−0.35 M NaCl over 12 min was used to elute the Ub variants, which were detected by absorbance at 494 nm. Quantification was based on a calibration curve of fluorescein-labeled Ub D77. The kinetic data were analyzed using OriginPro and fit to the Michaelis−Menten equation.

Autoubiquitination Assay.

Autoubiquitination reactions were performed at RT in a buffered solution containing 50 mM HEPES pH8.0 and 1 mM EDTA. For monoubiquitination reaction, 15 μM of the Yuh1 variant (wild type, T163K, Yuh1m, or Yuh1qm) was used along with 200 μM of Ub D77; for diubiquitination reaction, 5 μM of Yuh1qm was reacted with 50 μM Ub chains with D77 at the proximal end. Reactions were quenched by boiling in SDS-loading dye at different time points. Western blot analysis was performed using the mouse anti-Ubiquitin (P4D1) antibody (Enzo Life Sciences) at a 1:1000 dilution. We used the IRDye 800CW goat antimouse (LI-COR Biosciences) at a 1:15000 dilution as the secondary antibody.

Mass Spectrometry Analysis of Autoubiquitination Reactions.

Autoubiquitination reactions were separated by SDS-PAGE using NuPAGE 12% Bis-Tris protein gels (ThermoFisher Scientific). The bands corresponding to monoubiquitinated Yuh1qm were excised and prepared for in-gel digestion with GluC at a 1:10 g/g ratio and trypsin at a 1:20 g/g ratio. K48 diubiquitinated Yuh1qm and K63 triubiquitinated Yuh1qm5.6 was purified by a size exclusion chromatography (50 mM Tris, pH 7.5, 300 mM NaCl, 1 mM DTT) or anionic exchange chromatography (50 mM Tris, pH 7.5, 1 mM DTT as equilibration buffer and 50 mM Tris, pH 7.5, 500 mM NaCl, 1 mM DTT as elution buffer) and lyophilized. The dry sample (0.35 μg/ul) was denatured for 1 h at RT in a solution containing 25 mM ammonium bicarbonate and 8 M urea. Digestion of di/triubiquitinated Yuh1 variants were performed under the same reaction conditions as described above.

Proteomic analysis was performed at the UMASS-Amherst Mass Spectrometry Center. Briefly, nanoLC-MS/MS was conducted in an Orbitrap FusionTribid mass spectrometer (ThermoFisher Scientific). Digested peptides were separated in a nanoLC column (Thermo Acclaim PepMap RSLC column, 75 μm × 15 cm) with an Easy-nLC 1000 chromatography system (ThermoFisher Scientific) using a linear gradient 0−50% buffer B (acetonitrile, 0.1% formic acid) over 50 min. The eluted peptides were analyzed with resolution of 60 000 and scan range of 350−2000 m/z. Tandem mass spectrometry was performed using collision-induced dissociation (CID) with a 35% collision energy. The MS data were analyzed using Proteome Discoverer(ThermoFisher Scientific, Version 2.2) and SEQUEST HT search engine.

Yeast Strain and Plasmid.

The Yuh1qm (and WT) gene was amplified from pET28b using $pCTyuh1f$ and $pCTyuh1r$ with Accura polymerase (Lucigen) and was double digested with NheI and *Bam*HI (New England Biolabs). The digested gene was cloned into pCT plasmid to generate a pCT-yuh1 construct. For yeast surface display, *Saccharomyces cerevisiae* strain EBY100 (MATa AGA1::GAL1AGA1::URA3 ura352 trp1 leu2delta200 his3delta200 pep4::HIS3 prbd1.6R can1 GAL) was used.

Yeast Growth and Induction.

Yeast were transformed using the Frozen EZ Yeast Transformation II kit (Zymo Research) and plated on tryptophan-deficient dropout media (SDCAA plates; 20 g/L dextrose, 6.7 g/L yeast nitrogen base, 5 g/L casamino acids, 5.4 g/L Na_2HPO_4,8.56 g/L $NaH_2PO_4.H_2O$, 15 g/L agar, 182 g/L sorbitol) for 2−4 days at 30 °C to identify successful transformants. Transformed EBY100 cells were grown in 5 mL of SDCAA (20 g/L dextrose, 6.7 g/L yeast nitrogen base, 5 g/L casamino acids, 5.4 g/L Na_2HPO_4, 8.56 g/L $NaH_2PO_4.H_2O$) media overnight at 30 °C. We then pelleted at least 5×10^7 cells and resuspended them in 5 mL of tryptophan deficient dropout media containing galactose (SGCAA media; 20 g/L galactose, 6.7 g/L yeast nitrogen base, 5 g/L casamino acids, 5.4 g/L Na_2HPO_4,8.56 g/L $NaH_2PO_4.H_2O$) for induction to occur overnight at 20 °C.

Validation of the Yeast Display Strategy.

We harvested 5×10^6 cells and washed them with PBSF buffer (0.1% (v/v) BSA in PBS buffer, pH 7.4). Cells were then labeled with chicken anti-HA (1:250 dilution in PBSF buffer) (Gallus Immunotech) for 30 min at RT. Labeled cells were washed with PBSF buffer, aspirated, and incubated with 50 μM of biotinylated Ub D77 in 50 μL PBSF buffer for 10 min at RT. Reactions were quenched with 5 μM of the pan-DUB inhibitor PR-619 (Selleck Chemicals). Because PR-619 is a reversible inhibitor, we also added it to the PBSF wash buffer. Ubiquitinated cells were simultaneously labeled with a goat, antichicken antibody conjugated to Alexa 647 (1:100 dilution in PBSF buffer) (Invitrogen), and streptavidin conjugated to Alexa 488 (1:100 dilution in PBSF buffer) (Invitrogen) for 15 min on ice in a shielded box. Cells were washed one last time with PBSF buffer and resuspended in the same buffer prior to performing flow cytometry on a BD LSR Fortessa X20. We counted cells based on both high expression levels of Yuh1 and high autoubiquitination efficiency.

Construction of the Yuh1qm Library.

The Yuh1qm gene was mutagenized using Mutazyme II, a commercially available error prone polymerase (Agilent Technologies). The primers were the same as those used to amplify the DNA library pool: pCT-yuh1f2 and pCT-yuh1r2. To prepare electrocompetent yeast cells, a 25 mL culture of EBY100 cells was grown to OD 1.5 and treated with 25 mM DTT for 15 min. Cells were then harvested, washed, and resuspended in 150 μL E buffer (10 mM tris, pH 7.5, 270 mM sucrose, 2 mM $MgCl_2$). Cells were transformed with 1 μg of the NheI and *Bam*HI digested plasmid and 4 μg of amplified DNA library pool through electroporation. Transformed cells were serial diluted and plated in -Trp dropout media for 2− 4 days to estimate the size of the library.

Selection of Yuh1qm Library Displayed on the Yeast Surface.

Five rounds of selection were carried out using fluorescent activated cell sorting (FACS) on a BD FACS ARIA II with 488 nm (530/30 bandpass collection filter) and 640 nm (670/30 band-pass filter) excitation lasers. For the first round of selection, 2×10^8 cells displaying the Yuh1qm library were harvested and washed with PBSF buffer. Aspirated cells were then incubated with biotinylated Ub D77 using the procedure described above. In the second round, 50 μM of biotinylated Ub D77 was incubated with 2×10^7 cells. In subsequent

rounds, 5×10^6 cells were harvested and reacted with 5, 0.5, and 0.1 μM of biotinylated Ub D77. The reaction time was 10 min for all selection rounds except round 5, which was 5 min. At the end of rounds three and five, plasmids were isolated from the enriched clones using a Zymoprep yeast plasmid miniprep kit (Zymo Research) and electroporated into DH10β cells. Individual colonies were grown, miniprepped, and sequenced using *pCTyuh1r2* to identify beneficial mutations for autoubiquitination.

Validation of Selected Clones through Autoubiquitination Assays.

Selected clones were amplified using the primers *Yuh1forNdeI* and *Yuh1revXhol*., cloned into pET28b, expressed, and purified using the procedure described above. For autoubiquitination, 1 μM of Yuh1qm variants was incubated with 2 μM Ub D77 in 50 mM HEPES, pH 8.0, 1 mM EDTA. Reaction progress was monitored by gel densitometry; gels were stained using SYPRO Ruby (Invitrogen) and scanned on a Typhoon FLA 9500 (GE Healthcare). Data analysis was performed on Image Studio Lite (LI-COR Biosciences). Data corresponding to the hydrolysis of the autoubiquitinated species were fit to an exponential decay curve on OriginPro.

DUB Assays with Anchored and Unanchored Ub Chains.

For maximum conversion of free ubiquitin chains into ubiquitinated Yuh1qm5.6, 5 μM of clone 5.6 was incubated with 2.5 μM ubiquitin chains (with Ub D77 as the proximal unit) for 30 s. Reactions were quenched with 1 mM NEM and buffered exchanged into Milli-Q water. The resulting solutions were used directly in DUB assays. For DUB assays, 0.5 μM of the USPs or 1 μM of OTUs were incubated with the free and anchored ubiquitin chains. Reaction progress was monitored by gel densitometry. For free ubiquitin chains, gels were stained with SYPRO Ruby or transferred and blotted with the P4D1 antiubiquitin antibody (1:1000 dilution in 3% BSA, 0.1% TWEEN; Enzo Life Sciences). For anchored ubiquitin chains, gels were transferred and blotted with anti-6X His tag antibody (1:1000 dilutions in 3% BSA,0.1% TWEEN; Abcam). All Western blots were imaged on Odyssey CLx imaging system (LI-COR biosciences). Data analysis was performed on Image Studio Lite.

Supplementary Material

Refer to Web version on PubMed Central for supplementary material.

ACKNOWLEDGMENTS

We thank S. Eyles (UMass Amherst) for assistance with high-resolution mass spectrometry. All mass spectrometry data were collected and analyzed at UMASS-Amherst Mass Spectrometry Center. We thank A. Burnside (UMass Amherst) for assistance with fluorescent-activated cell sorting. All FACS data were collected using Flow Cytometry Core Facility at UMass Amherst. We thank S. Moore (Smith College) for kindly sharing EBY100 yeast cells and the pCT plasmid and for helpful discussions. This work was funded by a grant from the National Institutes of Health (RO1GM110543). The data described herein were acquired on an Orbitrap Fusion mass spectrometer funded by a grant from National Institutes of Health (1S10OD010645–01A1).

REFERENCES

(1). Hershko A, and Ciechanover A (1998) The Ubiquitin System. Annu. Rev. Biochem 67, 425–479. [PubMed: 9759494]

(2). Popovic D, Vucic D, and Dikic I (2014) Ubiquitination in Disease Pathogenesis and Treatment. Nat. Med 20, 1242–1253. [PubMed: 25375928]

(3). Pickart CM (2001) Mechanisms Underlying Ubiquitination. Annu. Rev. Biochem 70, 503–533. [PubMed: 11395416]

(4). Witting KF, Mulder MPC, and Ovaa H (2017) Advancing Our Understanding of Ubiquitination Using the Ub-Toolkit. J. Mol. Biol 429, 3388–3394. [PubMed: 28410891]

(5). van Tilburg GBA, Elhebieshy AF, and Ovaa H (2016) Synthetic and Semi-Synthetic Strategies to Study Ubiquitin Signaling. Curr. Opin. Struct. Biol 38, 92–101. [PubMed: 27315041]

(6). Pham GH, and Strieter ER (2015) Peeling Away the Layers of Ubiquitin Signaling Complexities with Synthetic Ubiquitin-Protein Conjugates. Curr. Opin. Chem. Biol 28, 57–65. [PubMed: 26093241]

(7). Mali SM, Singh SK, Eid E, and Brik A (2017) Ubiquitin Signaling: Chemistry Comes to the Rescue. J. Am. Chem. Soc 139, 4971–4986.

(8). Buetow L, and Huang DT (2016) Structural Insights into the Catalysis and Regulation of E3 Ubiquitin Ligases. Nat. Rev. Mol. Cell Biol 17, 626–642. [PubMed: 27485899]

(9). Mevissen TET, and Komander D (2017) Mechanisms of Deubiquitinase Specificity and Regulation. Annu. Rev. Biochem 86, 159–192. [PubMed: 28498721]

(10). Husnjak K, and Dikic I (2012) Ubiquitin-Binding Proteins: Decoders of Ubiquitin-Mediated Cellular Functions. Annu. Rev. Biochem 81, 291–322. [PubMed: 22482907]

(11). Hemantha HP, Bavikar SN, Herman-Bachinsky Y, Haj-Yahya N, Bondalapati S, Ciechanover A, and Brik A (2014) Nonenzymatic Polyubiquitination of Expressed Proteins. J. Am. Chem. Soc 136, 2665–2673. [PubMed: 24437386]

(12). Haj-Yahya M, Fauvet B, Herman-Bachinsky Y, Hejjaoui M, Bavikar SN, Karthikeyan SV, Ciechanover A, Lashuel HA, and Brik A (2013) Synthetic Polyubiquitinated α-Synuclein Reveals Important Insights into the Roles of the Ubiquitin Chain in Regulating Its Pathophysiology. Proc. Natl. Acad. Sci. U. S. A 110, 17726–17731. [PubMed: 24043770]

(13). Schaefer JB, and Morgan DO (2011) Protein-Linked Ubiquitin Chain Structure Restricts Activity of Deubiquitinating Enzymes. J. Biol. Chem 286, 45186–45196. [PubMed: 22072716]

(14). Chatterjee C, McGinty RK, Pellois JP, and Muir TW (2007) Auxiliary-Mediated Site-Specific Peptide Ubiquitylation. Angew. Chem., Int. Ed 46, 2814–2818.

(15). Ajish Kumar KS, Haj-Yahya M, Olschewski D, Lashuel HA, and Brik A (2009) Highly Efficient and Chemoselective Peptide Ubiquitylation. Angew. Chem., Int. Ed 48, 8090–8094.

(16). Kumar KSA, Spasser L, Erlich LA, Bavikar SN, and Brik A (2010) Total Chemical Synthesis of Di-Ubiquitin Chains. Angew. Chem., Int. Ed 49, 9126–9131.

(17). El Oualid F, Merkx R, Ekkebus R, Hameed DS, Smit JJ, De Jong A, Hilkmann H, Sixma TK, and Ovaa H (2010) Chemical Synthesis of Ubiquitin, Ubiquitin-Based Probes, and Diubiquitin. Angew. Chem., Int. Ed 49, 10149–10153.

(18). Virdee S, Ye Y, Nguyen DP, Komander D, and Chin JW (2010) Engineered Diubiquitin Synthesis Reveals Lys29-Isopeptide Specificity of an OTU Deubiquitinase. Nat. Chem. Biol 6, 750–757. [PubMed: 20802491]

(19). Virdee S, Kapadnis PB, Elliott T, Lang K, Madrzak J, Nguyen DP, Riechmann L, and Chin JW (2011) Traceless and Site-Specific Ubiquitination of Recombinant Proteins. J. Am. Chem. Soc 133, 10708–10711. [PubMed: 21710965]

(20). Madrzak J, Fiedler M, Johnson CM, Ewan R, Knebel A, Bienz M, and Chin JW (2015) Ubiquitination of the Dishevelled DIX Domain Blocks Its Head-to-Tail Polymerization. Nat. Commun 6, 6718. [PubMed: 25907794]

(21). Bang D, Makhatadze GI, Tereshko V, Kossiakoff AA, and Kent SB (2005) Total Chemical Synthesis and X-Ray Crystal Structure of a Protein Diastereomer: [D-Gln35]Ubiquitin. Angew. Chem., Int. Ed 44, 3852–3856.

(22). Yan LZ, and Dawson PE (2001) Synthesis of Peptides and Proteins without Cysteine Residues by Native Chemical Ligation Combined with Desulfurization. J. Am. Chem. Soc 123, 526–533.\ [PubMed: 11456564]

(23). Xu S, Patel P, Abbasian M, Giegel D, Xie W, Mercurio F, and Cox S (2005) In Vitro SCFβ-Trcp1-Mediated IκBα Ubiquitination Assay for High-Throughput Screen. Methods Enzymol 399, 729–740. [PubMed: 16338392]

(24). Saeki Y, Isono E, and Toh-E A (2005) Preparation of Ubiquitinated Substrates by the PY Motif-Insertion Method for Monitoring 26S Proteasome Activity. Methods Enzymol 399, 215–227. [PubMed: 16338358]

(25). Bhattacharyya S, Renn JP, Yu H, Marko JF, and Matouschek A (2016) An Assay for 26S Proteasome Activity Based on Fluorescence Anisotropy Measurements of Dye-Labeled Protein Substrates. Anal. Biochem 509, 50–59. [PubMed: 27296635]

(26). Akimov V, Barrio-Hernandez I, Hansen SVF, Hallenborg P, Pedersen A-K, Bekker-Jensen DB, Puglia M, Christensen SDK, Vanselow JT, Nielsen MM, Kratchmarova I, Kelstrup CD, Olsen JV, and Blagoev B (2018) UbiSite Approach for Comprehensive Mapping of Lysine and N-Terminal Ubiquitination Sites. Nat. Struct. Mol. Biol 25, 631–640. [PubMed: 29967540]

(27). Leznicki P, and Kulathu Y (2017) Mechanisms of Regulation and Diversification of Deubiquitylating Enzyme Function. J. Cell Sci 130, 1997–2006. [PubMed: 28476940]

(28). Valkevich EM, Guenette RG, Sanchez NA, Chen Y-C, Ge Y, and Strieter ER (2012) Forging Isopeptide Bonds Using Thiol-Ene Chemistry: Site-Specific Coupling of Ubiquitin Molecules for Studying the Activity of Isopeptidases. J. Am. Chem. Soc 134, 6916–6919. [PubMed: 22497214]

(29). Trang VH, Valkevich EM, Minami S, Chen Y-C, Ge Y, and Strieter ER (2012) Nonenzymatic Polymerization of Ubiquitin: Single-Step Synthesis and Isolation of Discrete Ubiquitin Oligomers. Angew. Chem., Int. Ed 51, 13085–13088.

(30). Trang VH, Rodgers ML, Boyle KJ, Hoskins AA, and Strieter ER (2014) Chemoenzymatic Synthesis of Bifunctional Polyubiquitin Substrates for Monitoring Ubiquitin Chain Remodeling. ChemBioChem 15, 1563–1568. [PubMed: 24961813]

(31). Johnston SC, Riddle SM, Cohen RE, and Hill CP (1999) Structural Basis for the Specificity of Ubiquitin C- Terminal Hydrolases. EMBO J 18, 3877–3887. [PubMed: 10406793]

(32). Ritorto MS, Ewan R, Perez-Oliva AB, Knebel A, Buhrlage SJ, Wightman M, Kelly SM, Wood NT, Virdee S, Gray NS, Morrice NA, Alessi DR, and Trost M (2014) Screening of DUB Activity and Specificity by MALDI-TOF Mass Spectrometry. Nat. Commun 5, 1–11.

(33). Ménard R, Carrière J, Laflamme P, Plouffe C, Khouri HE, Storer AC, Carrière J, Khouri HE, Vernet T, Tessier DC, Thomas DY, and Storer AC (1991) Contribution of the Glutamine 19 Side Chain to Transition-State Stabilization in the Oxyanion Hole of Papain. Biochemistry 30, 8924–8928. [PubMed: 1892809]

(34). Chao G, Lau WL, Hackel BJ, Sazinsky SL, Lippow SM, and Wittrup KD (2006) Isolating and Engineering Human Antibodies Using Yeast Surface Display. Nat. Protoc 1, 755–768.

(35). Chen TF, De Picciotto S, Hackel BJ, and Wittrup KD Engineering Fibronectin-Based Binding Proteins by Yeast Surface Display, 1st ed.; Elsevier Inc., 2013; Vol. 523.

(36). Edelmann MJ, Iphofer A, Akutsu M, Altun M, di Gleria K, Kramer HB, Fiebiger E, Dhe-Paganon S, and Kessler BM (2009) Structural Basis and Specificity of Human Otubain 1-Mediated Deubiquitination. Biochem. J 418, 379–390.

(37). Wiener R, Dibello AT, Lombardi PM, Guzzo CM, Zhang X, Matunis MJ, and Wolberger C (2013) E2 Ubiquitin-Conjugating Enzymes Regulate the Deubiquitinating Activity of OTUB1. Nat. Struct. Mol. Biol 20, 1033–1039. [PubMed: 23955022]

(38). Mevissen TET, Hospenthal MK, Geurink PP, Elliott PR, Akutsu M, Arnaudo N, Ekkebus R, Kulathu Y, Wauer T, El Oualid F, Fruend SM, Ovaa H, and Komander D (2013) OTU Deubiquitinases Reveal Mechanisms of Linkage Specificity and Enable Ubiquitin Chain Restriction Analysis. Cell 154, 169–184. [PubMed: 23827681]

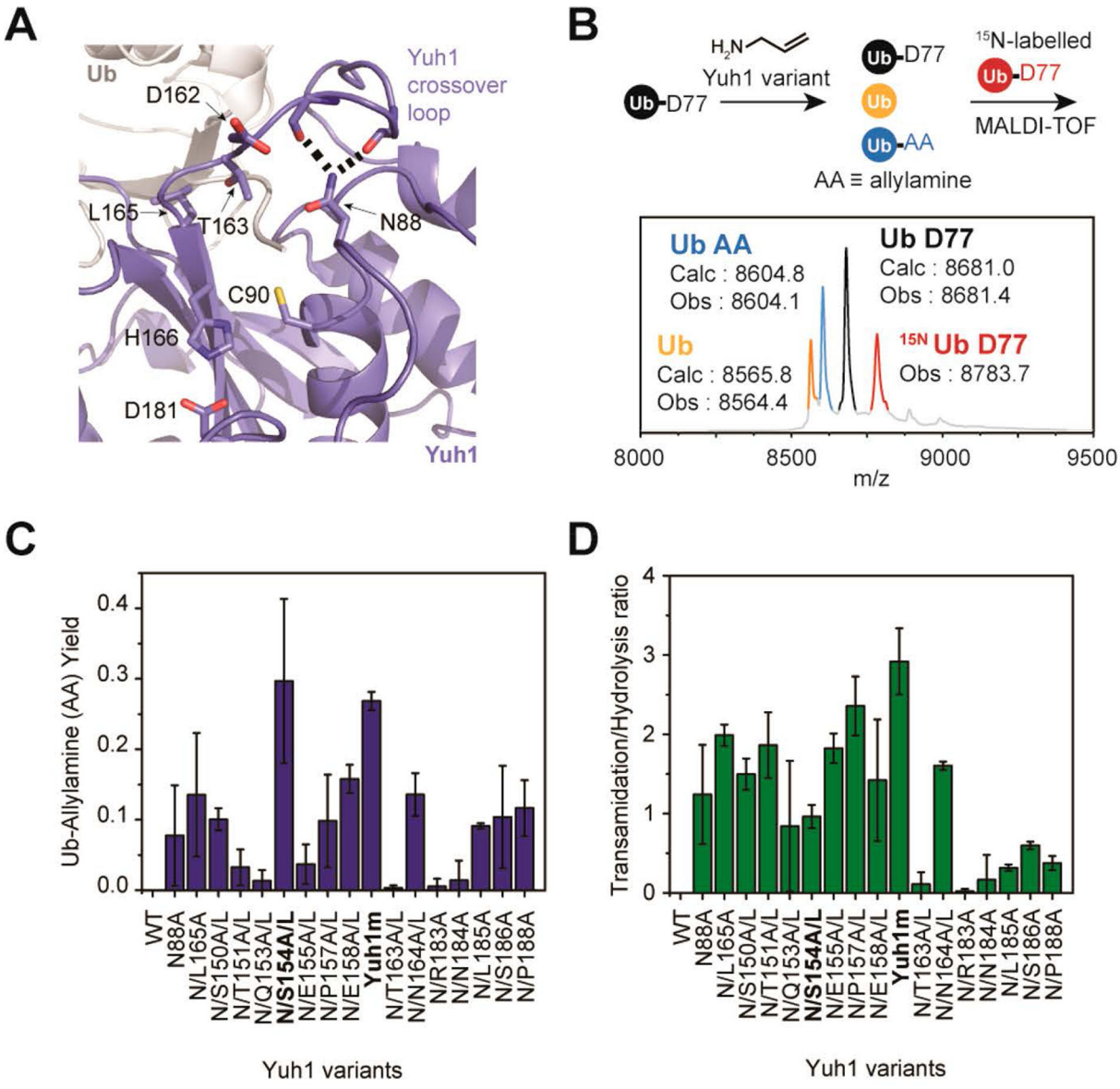

Figure 1.

Targeted mutagenesis of Yuh1. (A) Structure (PDB: 1CMX[31]) shows the catalytic triad of Yuh1 (C90, H166, and D181) with C90 covalently attached to the C-terminus of Ub. N88 forms hydrogen bonds with residues in the flexible crossover loop. (B) MALDI-TOF assay for monitoring transamidation and hydrolysis. Yuh1 variants were used to transform Ub D77 into the transamidated product, Ub-allylamine (Ub AA), and wild type Ub. Products were quantified using MALDI-TOF MS and ^{15}N-labeled Ub D77 as an internal standard. (C) Yield of Ub-allylamine after 1 h in the presence of Yuh1 variants and Ub D77. Error bars correspond to standard deviation of two biological replicates and two technical replicates. (D) Transamidation to hydrolysis ratio for each Yuh1 variant, as determined by MALDI-TOF MS. Error bars correspond to standard deviation of two biological replicates and two technical replicates.

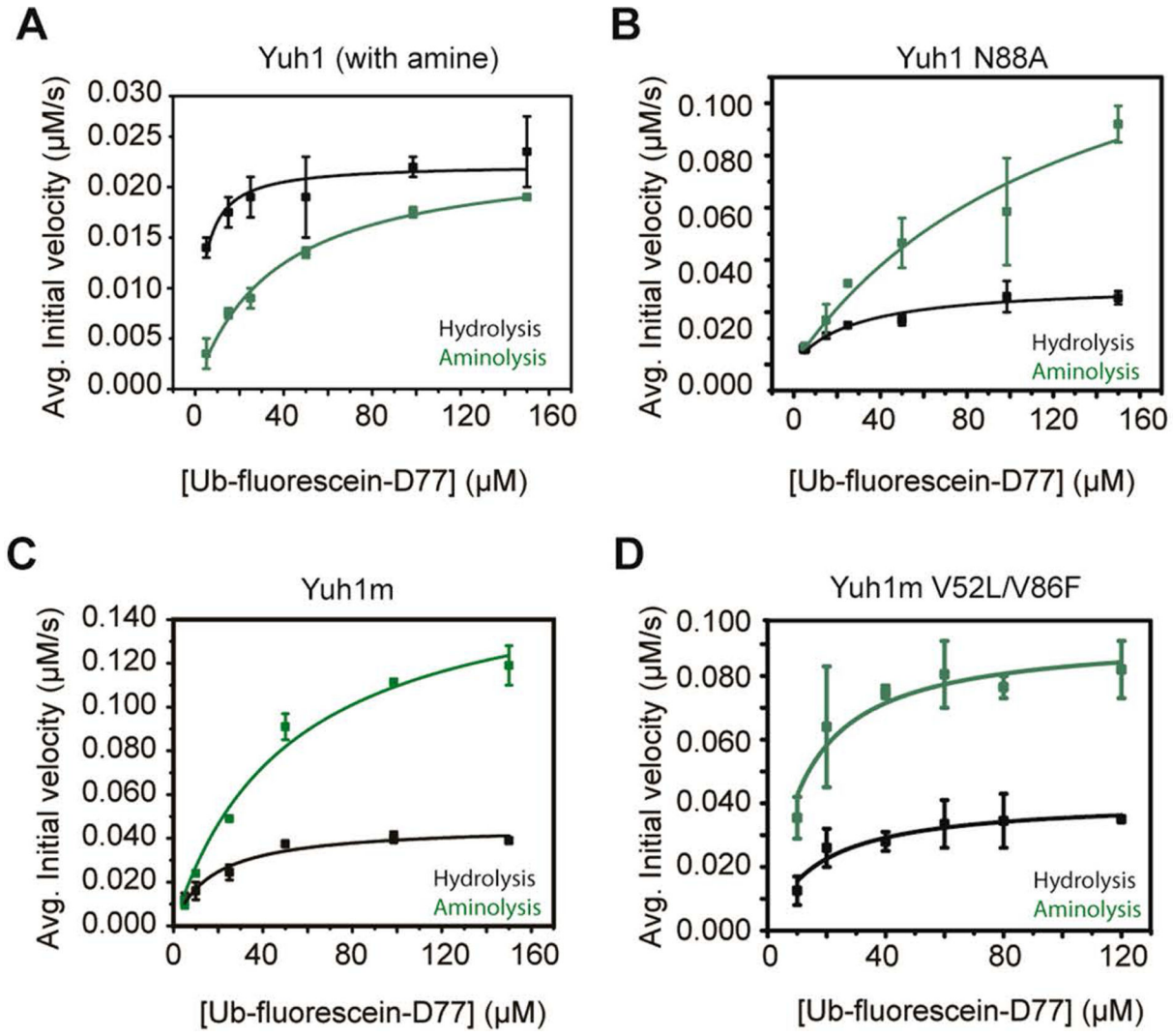

Figure 2.

Steady-state kinetic analysis of transamidation and hydrolysis. Michaelis−Menten plot for the transamidation and hydrolysis of Ub D77 with allylamine and (A) wild type Yuh1, (B) Yuh1 N88A, (C) Yuh1m, and (D) Yuh1m V52L/V86F. Error bars correspond to the standard error from two biological replicates.

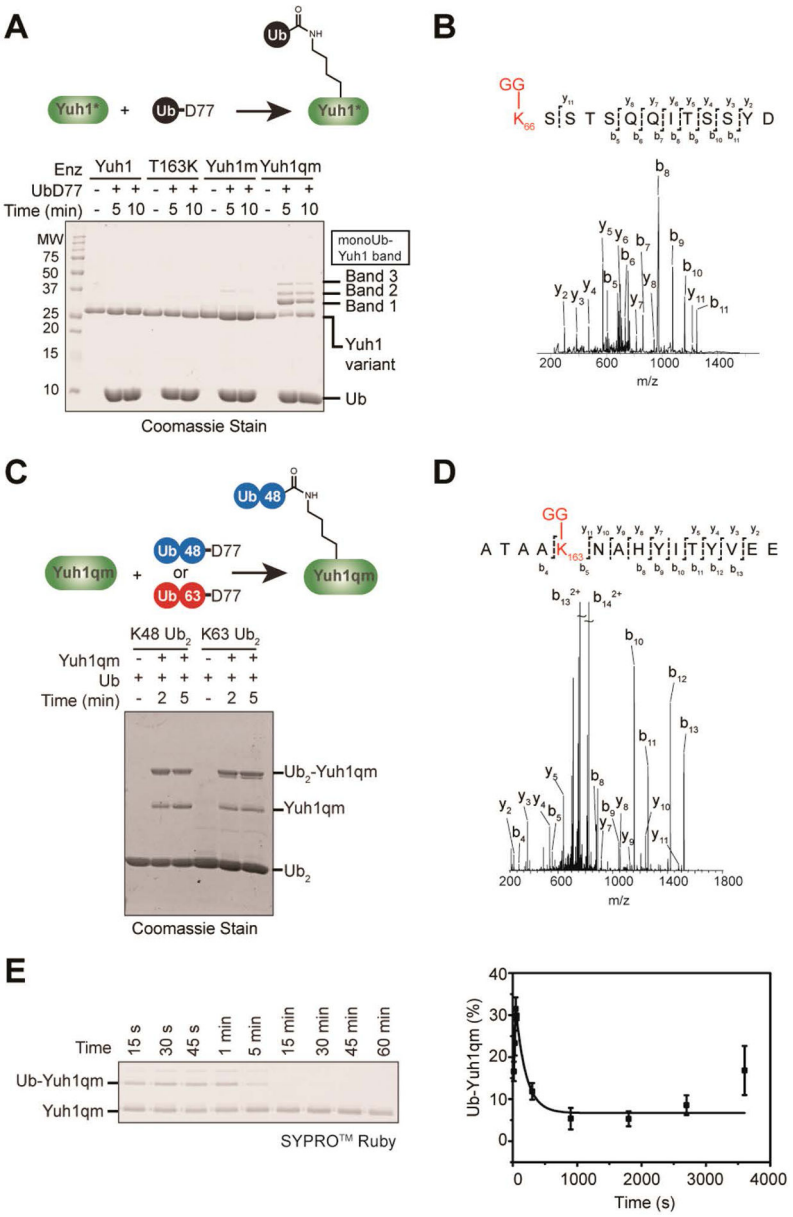

Figure 3.

Autoubiquitination of Yuh1 variants. (A) SDS-PAGE analysis of autoubiquitination with Yuh1 variants (15 μM) and Ub D77 (200 μM). Bands 1−3 correspond to monoubiquitinated Yuh1 variants. (B) MS/MS spectrum showing ubiquitination at K66 of Yuh1qm. (C) SDS-PAGE analysis of Yuh1qm (5 μM) autoubiquitination with Ub dimers (50 μM). (D) MS/MS spectrum showing diubiquitination at K163 of Yuh1qm. (E) SDS-PAGE analysis of the autohydrolysis of monoubiquitinated Yuh1qm. The monoubiquitinated product (Ub-Yuh1qm) was generated from Yuh1qm (1 μM) and Ub D77 (2 μM). Hydrolysis data were fit to a single exponential decay ($t_{1/2}$ = 160 ± 60 s). Error bars correspond to the standard error from three biological replicates.

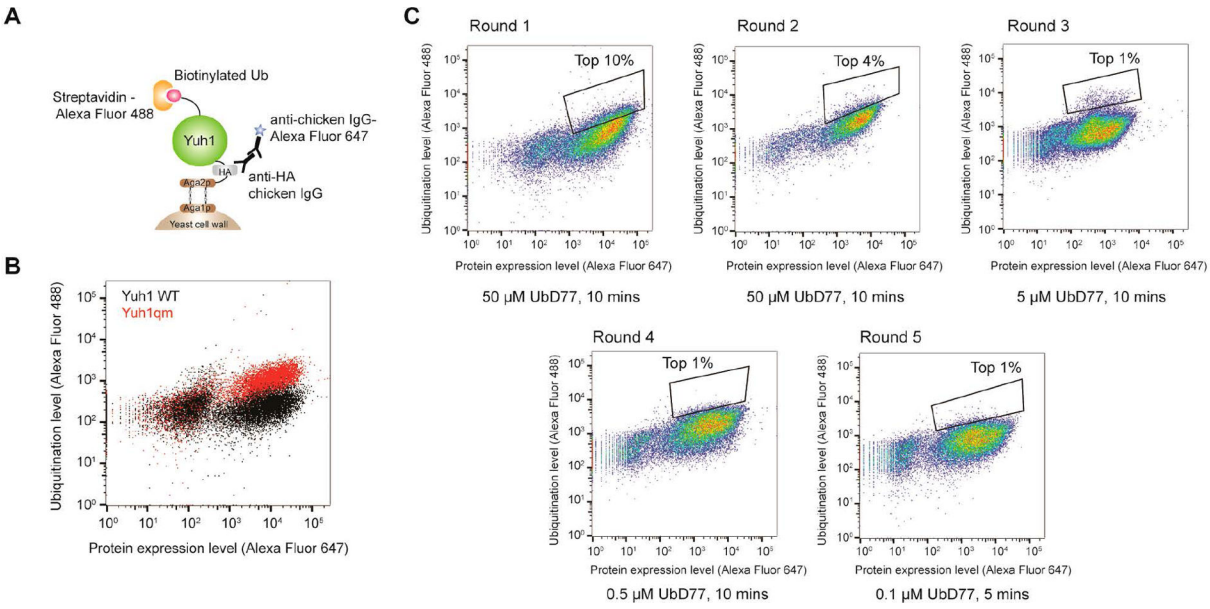

Figure 4.

Yeast selection of the Yuh1qm library. (A) Yeast cell surface display of Yuh1qm variants and selection of library members based on the transfer of biotinylated ubiquitin to a Lys residue. Biotinylated ubiquitin attached to a Yuh1 variant is labeled with streptavidin-Alexa 488, and the HA-tag fused to the N-terminus of Yuh1 variants is labeled with a chicken anti-HA antibody and an antichicken IgG conjugated with Alexa 647. (B) FACS of wild type Yuh1 and Yuh1qm using biotinylated ubiquitin D77. Cells are double labeled with streptavidin-Alexa 488 and Alex 647. (C) FACS of the Yuh1qm library to select for cells doubly labeled with streptavidin-Alexa 488 and Alex 647. The Yuh1qm library underwent five rounds of biotinylated ubiquitin labeling, streptavidin and antibody labeling, and cell sorting. The frames and percentages in black designate the fraction of yeast cells collected by FACS in each round of selection.

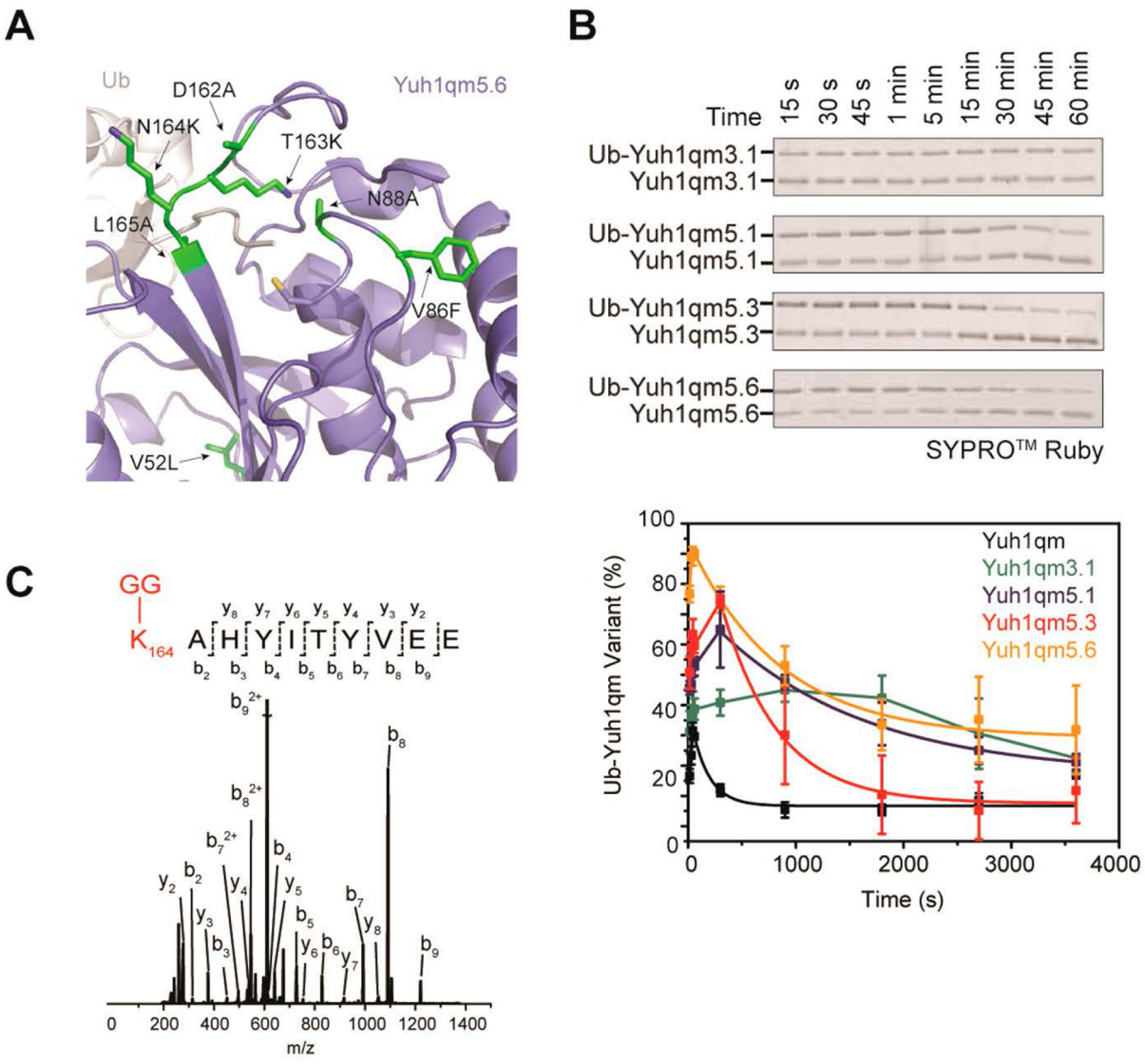

Figure 5.

Autoubiquitination of evolved Yuh1 variants. (A) Structure shows the mutated residues in Yuh1qm5.6. (B) SDS-PAGE analysis of the autohydrolysis of mono-Ub-Yuh1qm variants. The monoubiquitinated products were generated from a Yuh1qm variant (1 μM) and Ub D77 (2 μM). Hydrolysis data were fit to a single exponential decay (Yuh1qm5.1, $t_{1/2}$ = 1400 ± 100 s; Yuh1qm5.3, $t_{1/2}$ = 500 ± 100 s; Yuh1qm5.6, $t_{1/2}$ = 800 ± 100 s). Error bars correspond to the standard error from three biological replicates. (C) MS/MS spectrum showing ubiquitination at K164 of Yuh1qm5.6.

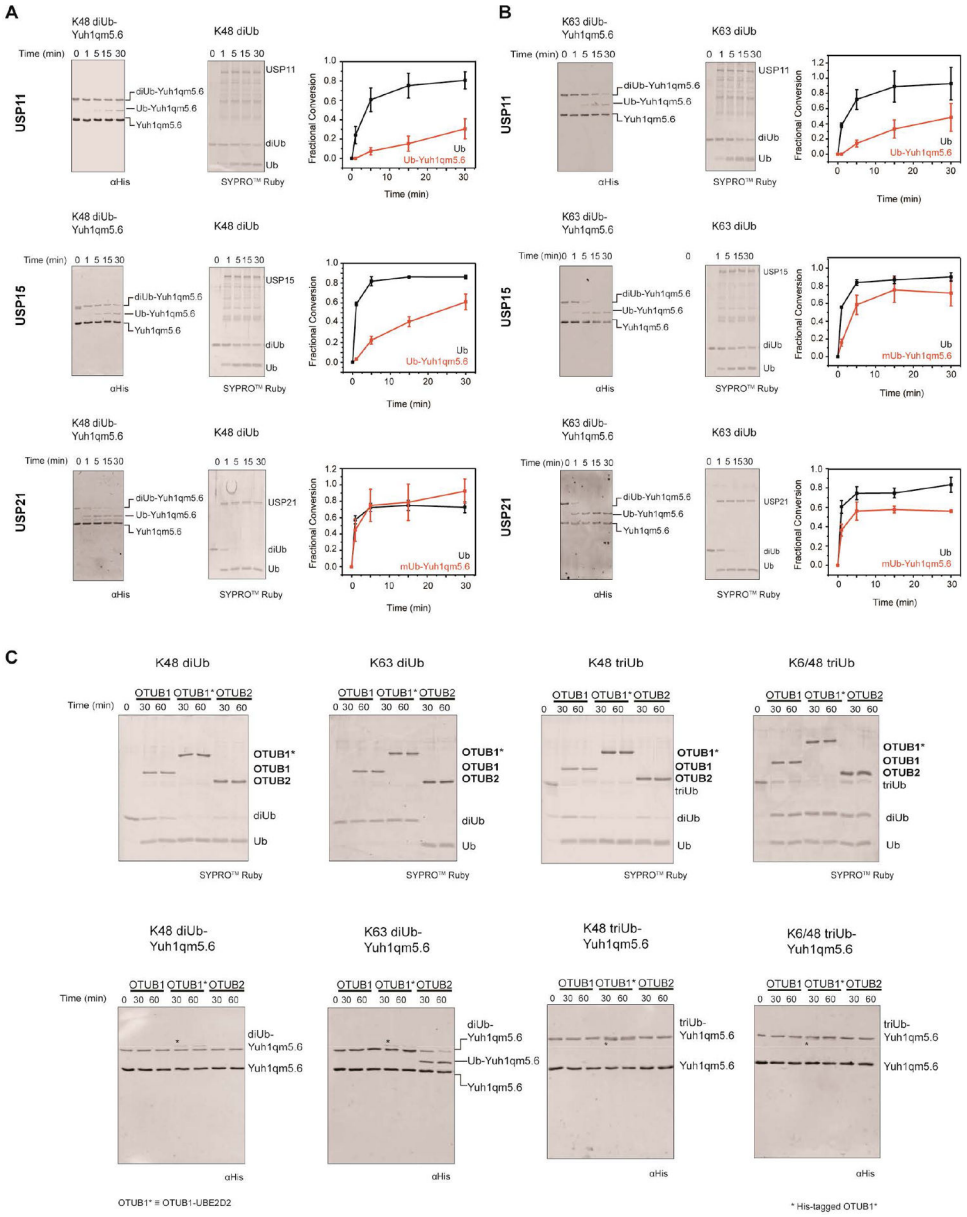

Figure 6.

DUB profiling with autoubiquitinated Yuh1qm5.6. (A) Cleavage of Yuh1qm5.6-anchored and unanchored K48 dimers by USP11, USP15, and USP21. Error bars correspond to the standard error of three biological replicates. (B) Cleavage of Yuh1qm5.6-anchored and unanchored K63 dimers by USP11, USP15, and USP21. Error bars correspond to the standard error of three biological replicates. (C) Cleavage of Yuh1qm5.6-anchored and unanchored chains by OTUB1, OTUB1*, and OTUB2, OTUB1*; OTUB1 fused to the E2 UBE2D2 (OTUB1-UBE2D2). The data shown here corresponds to Yuh1qm5.6-anchored and unanchored chains that were treated with NEM to prevent hydrolysis.

Table 1.

Steady-State Kinetic Parameters for Hydrolysis and Transamidation with Yuh1 Variants

	hydrolysis			transamidation		
	$K_m(\mu M)$	$k_{cat}(s^{-1})$	$k_{cat}/K_m(M^{-1}\ s^{-1})$	$K_m(\mu M)$	$k_{cat}(s^{-1})$	$k_{cat}/K_m(M^{-1}\ s^{-1})$
Yuhl (no amine)	5 ± 2	3.1 ± 0.2	$6 \pm 3 \times 10^5$			
Yuhl	4 ± 1	3.0 ± 0.1	$8 \pm 2 \times 10^5$	36 ± 4	3.1 ± 0.1	$9 \pm 1 \times 10^4$
YuhlN88A	27 ± 7	0.062 ± 0.006	$2.3 \pm 0.6 \times 10^3$	130 ± 60	0.32 ± 0.08	$3 \pm 1 \times 10^3$
Yuhlm	17 ± 4	0.092 ± 0.006	$5 \pm 1 \times 10^3$	51 ± 11	0.34 ± 0.02	$6 \pm 2 \times 10^3$
Yuhlm VS2L/V86F	16 ± 4	0.082 ± 0.006	$5 \pm 1 \times 10^3$	12 ± 3	0.19 ± 0.02	$16 \pm 2 \times 10^3$